
INTERFEROMETRY AND POLARIMETRY FOR OPTICAL SENSING

JULIAN D. C. JONES
*Heriot-Watt University
Edinburgh, UK*

Abstract

When the highest measurand sensitivity is required, interferometric techniques are appropriate. The general principles, techniques and some applications of interferometry and polarimetry useful in optical sensing technology are addressed and discussed in this chapter.

12.1 Introduction

Optical interferometry has long been associated with precision metrology, and is the basis by which the fundamental length standard is transferred to practical measurements. An optical interferometer is an instrument in which two or more optical path lengths may be compared; when mutually coherent beams of light corresponding to two different paths fall on a square-law detector, then the resultant intensity varies with the relative path difference with a period equal to the optical wavelength. Thus, optical path lengths can be measured on the scale of the wavelength of light.

The advent of single-mode optical fibre and related components has made it possible to construct interferometers that are sufficiently robust to be used in applications beyond the metrology laboratory. Fibre optic interferometers are now the basis of a wide range of new kinds of measuring instruments. This chapter is concerned with the sensors in which the transduction principle is the modulation of the optical path length of a fibre sensing element in response to the measurand. The optical path change is measured by interferometry and the measurand is hence revealed.

It is now more than 25 years since the connection between the optical path length of a fibre-

guided mode and the physical environment was first recognised, during research into coherent optical communication systems. There quickly followed the realisation that the environmental-dependence of path length in single-mode optical fibres could be used to measure temperature and strain. The earliest major research programme on optical fibre sensors was for applications in acoustic pressure sensing, in hydrophones. The contemporary development of the optical fibre gyroscope is described in Chapter 16 of this book.

Closely related to interferometric sensors are those based on polarimetry. A polarimetric sensor is one in which the measurand controls the state of polarisation of the guided beam. That state can be considered as a superposition of two orthogonal polarisation eigenstates. In many polarimetric sensors the transduction mechanism is the modulation of the optical phase difference between the eigenstates. Such sensors are therefore directly analogous to interferometers (see Chapter 27).

12.2 General Principles

An optical sensor may be formally defined as a device in which an optical signal is modulated in response to a measurand field. Let us assume that the source has some well-defined wavelength spectrum, and that the electric field at wavelength λ is $E(\lambda)$ in unit bandwidth. If the corresponding received electric field is $E'(\lambda)$, then

$$E'(\lambda) = T(X, \lambda)E(\lambda) \quad (12.1)$$

where $T(X, \lambda)$ is the propagation matrix describing the sensing element and X is a vector describing the physical environment, including terms representing temperature, stress, and electromagnetic fields. The function of the signal processing used in the sensor system is to invert (Figure 12.1) to find T , invert again to find X , and then to identify and evaluate the relevant component(s) of X to recover the desired measurand. We shall see that in an interferometric sensor the effect of the measurand is to modulate the *phase* of the electric field, where phase is converted to an intensity change in the interferometer.

It is instructive to express T as a product of terms, each describing a physically observable effect on the transmitted beam, such that

$$T = ae^{i\phi_1} B \quad (12.2)$$

where a is the scalar transmittance, ϕ_1 the mean phase retardation and B the birefringence matrix of the element; a , ϕ_1 , and B are all both dispersive and environmentally sensitive.

In single-mode fibres, sensing mechanisms based on modulation of any one or a combination of the parameters a , ϕ_1 , and B are feasible. In practice, however, the transmittance shows only weak environmental sensitivity, and sensors are thus generally based on phase and polarisation modulation, recovered using interferometry and polarimetry respectively. It is necessary to consider only the ellipticity and azimuth of the state of polarisation of the guided beam so that the polarisation properties of the guiding medium may be adequately described by a 2×2 unitary complex matrix – the Jones matrix [1]. Hence we may describe the transfer function of a single-mode sensing element by

$$E' = a_0 E e^{i\phi_1} B \quad (12.3)$$

where a_o is a scalar constant (the transmittance) and B is the Jones matrix.

For a fibre possessing perfect cylindrical symmetry, B becomes the identity matrix I , but in general it is necessary to consider the effects of birefringence within the fibre. For example, for a linearly birefringent fibre

$$B = B_l \begin{bmatrix} e^{i\phi_2/2} & 0 \\ 0 & e^{-i\phi_2/2} \end{bmatrix} \quad (12.4)$$

Such a fibre is characterised by two linear polarisation eigenmodes, such that ϕ_2 is the induced relative phase retardation between the eigenmodes caused by propagation through the fibre. For a circularly birefringent fibre

$$B = B_c = \begin{bmatrix} \cos \phi_3 & -\sin \phi_3 \\ \sin \phi_3 & \cos \phi_3 \end{bmatrix} \quad (12.5)$$

where $2\phi_3$ is the induced relative phase retardation between the eigenmodes, which in this case are left and right circularly polarised states.

It is therefore possible to characterise the fibre in terms of the three phase constants ϕ_1 , ϕ_2 , and ϕ_3 . They are dependent on the material properties and geometry of the fibre, and also on the physical environment. These phase sensitivities may be exploited either to form fibre optic sensing elements, or as the basis of phase or polarisation state modulators. The environmental sensitivity of the fibre may be expressed in terms of dependence of the ϕ_i ($i = 1, 2, 3$) on external stimuli such as temperature (T), pressure (P) and strain ($\Delta l/l$), such that

$$\frac{\partial \phi_i}{\partial X} = \frac{2\pi}{\lambda} \left(n_i \frac{\partial l}{\partial X} + l \frac{\partial n_i}{\partial X} \right) ; \quad X = T, P, \Delta l, \dots ; \quad i = 1, 2, 3 \quad (12.6)$$

where l is the length of the fibre; n_i is the effective index of the fibre; n_2 is the difference between the refractive indices for the two orthogonal linear polarisation states, and n_3 is the difference for the orthogonal circular states. The first term within the brackets corresponds to the physical extension of the fibre, and the second to changes in the various terms in the refractive index [2,3].

The first single-mode fibre intrinsic sensors were true interferometers, in which light from the source was divided to follow two (or more) fibre-guided paths. The beams were then recombined to mix coherently together. From the intensity observed at the output from the interferometer, the phase difference between the optical paths, ϕ_1 , may be determined. Instruments such as these are termed *interferometric*, and for optimum performance the states of polarisation of the recombining beams should be equivalent. Most fibre interferometers are two beam devices in which one fibre is exposed to the measurand (the final fibre) and the other is isolated from it (the reference fibre).

Consider an optical fibre strain gauge. For simplicity, it is assumed that the sensing element is a length of nominally cylindrically symmetrical fibre with no birefringence. It is assumed also that the measurand is a purely axial strain, with no transverse components. The application of strain to the fibre has three effects: firstly, the fibre is physically extended; secondly, the strain modifies the refractive index of the fibre core; and thirdly the dimensions of the core are modified. The first effect is the dominant one, and if the others were negligible then increasing the length of the fibre by one wavelength would produce an optical path difference change of one

wavelength in the interferometer. However, the second effect is about 20 % as large as the first in fused silica and is of opposite sign to the first, thus *reducing* slightly the sensitivity. The third effect is more complicated. The effective refractive index of the guided mode lies between that of the core material and the cladding material, and in practical fibres is close to that of the core. Reducing the diameter of the core pushes the effective index closer to that of the cladding. Thus increasing axial strain reduces the effective index. However, for practical fibres the third effect is negligible. Thus a typical overall strain sensitivity for a fibre at a wavelength of 633 nm would be about 6.5×10^6 rad/m [4].

An analogous argument applies to temperature sensitivity where there are again three effects: thermal expansion of the fibre length; modification of the core index via the thermo-optic effect; and thermal expansion of the core radius. In fused silica the thermal expansivity is small, and it is the second term which is dominant. The third term is negligible. A typical overall thermal sensitivity at 633 nm is 100 rad/K for a 1 m sensing element length [5].

One can go on to derive the sensitivity of the fibre to other measurands. For example, the effect of pressure on the fibre is to reduce the physical length and diameter, and to modify the refractive index via the strain-optic effect [6].

The function of an interferometer is to transduce phase changes to intensity changes. However, the transfer function in the simplest case is periodic, with period 2π radians. Thus a challenge in the design of signal processing systems is to recover the phase free of the ambiguity imposed by the periodicity.

For normal fibres with nominal circular symmetry, the polarisation terms ϕ_2 and ϕ_3 are relatively insensitive to the environment, so that such fibre is not generally useful for polarisation-based sensing purposes. However, *highly birefringent* fibres have been commercially available for many years [7], and are well-suited to many sensing applications based on the modulation of ϕ_2 (polarisation ellipticity). The response of such a fibre to strain or temperature depends on the structure of the fibre, and in particular how the birefringence is induced. For the fibre in the above reference, the birefringence is induced by thermal stress. The fibre is made from a preform where the cladding contains sectors of different coefficient of thermal expansion than the surrounding main cladding material. Thus when the fibre cools down after drawing, considerable anisotropic stress is set up across the core.

Consider the application of such a fibre for temperature measurement [8]. The fibre can be visualised as guiding two linear polarisation eigenmodes of azimuth aligned to the principal stress directions, e.g. the horizontal and vertical states of polarisation, with distinct effective refractive indices. When the temperature changes, so does the physical length of the fibre. Because the refractive indices of the two modes are different, there is a small change in their *relative* path length. A much larger effect is caused by the change in stress distribution generated by the temperature change, thus changing the difference between the effective refractive indices of the two modes. Thus the sensitivity of such a sensing element is strongly dependent on the structure of the fibre. One parameter describing the structure is the *polarisation beat length* [9] which is the distance over which a path difference of one wavelength accumulates between the polarisation eigenmodes. For a thermally-stressed fibre of the type described above having a beat length of about 3 mm, a typical thermal sensitivity would be about 5 rad/K for a 1 m sensing length [10].

A similar argument applies to polarimetric strain measurement. Here, the strain modifies the

relative refractive index of the eigenmodes as well as producing a physical extension of the fibre [11]. It is the changing relative index that dominates.

Sensors have been developed which are based on the modulation of ϕ_3 ; that is, devices in which the measurand controls the circular birefringence of the sensing element, thus producing a rotation in the polarisation azimuth of the guided beam. The most important class of circular birefringence sensor is formed by those based on Faraday rotation [12] for the measurement of magnetic fields (see Chapter 27). However, sensors based on circular birefringence modulation have been demonstrated for other measurands. For example, Langeac [13] has reported a thermometer in which the sensing element was a length of single-mode fibre which had been twisted to induce a relatively high degree of circular birefringence.

12.3 Interferometry

It was shown in the previous section that in single-mode systems a range of physical measurands can be transduced to phase or polarisation modulations, expressible in terms of three phase constants. An interferometer converts a phase change to an intensity change. The simplest kind of interferometry to visualise is an optical arrangement that causes two mutually coherent beams of light to follow physically distinct paths. One of those paths contains the sensing fibre and the other path is used as a reference. When the two beams are combined on a non-linear detector then they produce a resultant intensity that changes periodically with the phase difference, with periodicity 2π . Such an arrangement is suitable for sensors based on the modulation of ϕ_1 , in the nomenclature of the analysis above. A polarimetric sensor can be thought of as one in which the two beams occupy essentially the same volume of space but are distinguished by the orthogonality of their states of polarisation. In order to make the two orthogonal states interfere on a non-linear detector, they must each be resolved to give components in a common direction. For example, by placing a polariser in the output of a highly birefringent fibre, the two modes are made to interfere provided that the azimuth of the polariser does not coincide with that of just one of the modes. All practical detectors of optical radiation are non-linear in that they respond to the *power* of the radiation rather than its electric field strength, averaged over some time period which is long in comparison with the period of an individual optical wavelength.

12.3.1 Two beam interferometers

A common form of optical fibre interferometer is the Mach-Zehnder configuration, with a simple example shown in Figure 12.1. The source is coupled into a single mode fibre downlead and is amplitude-divided into two fibre arms, which can be thought of as representing a *signal* beam and a *reference* beam, the measurand modifies the phase of the signal beam, whereas the reference beam enjoys a constant environment. The two beams then recombine at a second directional coupler (DC) into two upleads terminating in photodetectors giving an electrical output proportional to the power incident upon them.

It can be shown [14] that the detector signals are given by:

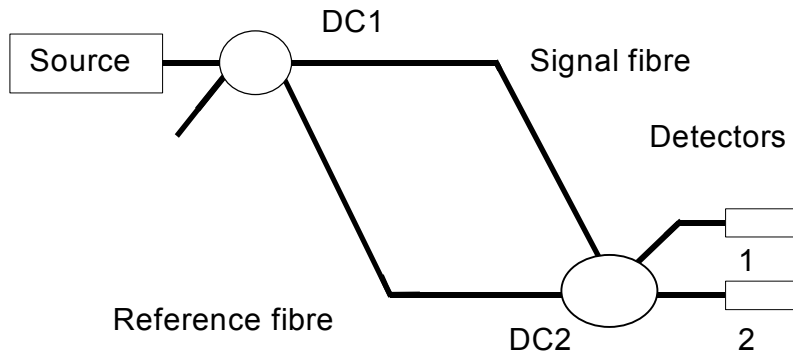


Figure 12.1 An optical fibre Mach-Zehnder interferometer.

$$I_1 = I_0[1 - V \cos(\phi_a - \phi_b)] \quad (12.7)$$

and

$$I_2 = I_0[1 + V \cos(\phi_a - \phi_b)] \quad (12.8)$$

where ϕ_a and ϕ_b are the phases for the signal and reference beams, I_0 is a mean signal level, and V is the *visibility* of the interference. Visibility depends on the relative intensity of the signal and reference beams, their relative states of polarisation, and their mutual coherence. In the optimum case, the relative intensities and states of polarisation are equal and the optical path length difference between the signal and reference beams is much smaller than the coherence length of the detected light. Good spatial coherence is intrinsic to the use of single-mode optical fibre. Under these optimum conditions, the visibility is unity. In practical circumstances the visibility can take any value between zero and unity. Notice that the two outputs are in *antiphase*, so that the sum of the two outputs is constant irrespective of relative phase. Having access to the two outputs can be used to compensate for the effect of changing source intensity.

The relative intensities of the two beams depend on the coupling coefficients of the directional couplers used, fixed during manufacture for those of fused type. The relative state of polarisation depends on the birefringence of the fibres and the couplers. Whilst it is possible to fabricate the entire interferometer from highly birefringent fibre and components, and to work with a fixed polarisation eigenstate, most interferometers are constructed from normal cylindrically-symmetric fibre. Thus environmental effects cause the recombining states to be unequal. Under these circumstances, some form of explicit birefringence control is needed to preserve visibility; one common means is to induce controlled birefringence by bending the fibre [15].

The coherence length is set by the bandwidth of the light at the detector, and is usually dominated by the properties of the source. The properties of interferometers illuminated with low coherence sources are considered further below.

Closely related to the Mach-Zehnder interferometer is Michelson's spectral interferometer, shown in Figure 12.2. Here, the signal and reference beams terminate in reflectors so that they are folded back on themselves to recombine at the same coupler that was used to divide them.

The double-pass of the signal beam effectively doubles the sensitivity of the interferometer.

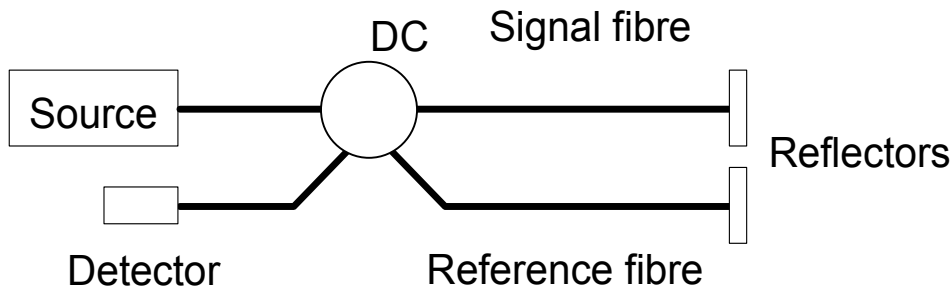


Figure 12.2 Fibre optic Michelson interferometer.

However, directing one of the interferometer outputs into the source is disadvantageous as such feedback causes instabilities [16], especially with diode lasers which are the source of choice for fibre sensors. In practical situations it is usually necessary to incorporate an optical isolator between the source and the coupler. The normal choice of isolator is of the Faraday type: a linearly polarised incident beam passes through an aligned polariser, and then via a magneto-optic crystal in a permanent magnetic field that rotates the polarisation azimuth by $\pi/4$ radians to be aligned with a polarisation analyser at the output. Thus, a counter-propagating (feedback) beam passing through the device will have its polarisation azimuth rotated in the crystal so that it cannot pass through the polariser. Difficulty of access to the antiphase output of the interferometer is also a disadvantage.

The recombining beams in the output arm of the Michelson interferometer are always of equal intensity, irrespective of the coupling ratio. However, the highest mean intensity is achieved for a 50:50 split ratio. Polarisation effects are similar to those in the Mach-Zehnder interferometer. However, there is an interesting means of ensuring equality of polarisation states without having to resort to an adjustable polarisation controller, in which the reflectors at the distal ends of the signal and reference fibres are replaced by '*Faraday mirrors*' [17]; these devices are essentially the same as Faraday isolators from which the polarisers have been removed.

Thus, the returning signal and reference beams are in the states orthogonal to those of the outgoing beams, so that they return to the coupler in the same states as when they left it, irrespective of any birefringence *en route*, thus optimising the visibility.

A special and important two-beam interferometer is the *Sagnac*, shown in Figure 12.3.

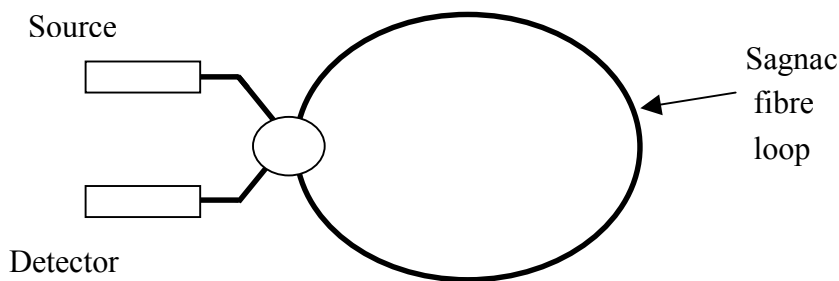


Figure 12.3 The fibre Sagnac interferometer.

The fibre Sagnac interferometer has been developed principally for the purpose of measuring angular velocity, as a *gyroscope* [18], and is considered in Chapters 16 and 28.

The signal and reference beams now occupy the same space, and are the clockwise and counter-clockwise beams propagating in the loop of fibre that forms the interferometer. At first sight it would appear that the phase difference between the beams would always be zero, as indeed it is for all *reciprocal* effects. However, non-reciprocal effects, such as angular velocity [19], magnetic fields [20] or dynamic measurands [21], all produce a phase shift. For example, consider the effect of a dynamic strain close to one end of the fibre loop. The counter-propagating beams returning to the detector at a given instant have ‘seen’ different values of the strain, and therefore exhibit a phase difference. Figure 12.3 shows the simplest possible version of the interferometer. In practice, it would be more usual for the source and detector to share the same download via an additional coupler, in order that the signal and reference beams would undergo more nearly reciprocal paths [22].

12.3.2 Polarimeters

Figure 12.4 shows a simple arrangement for a polarimetric sensor, which is closely analogous to the two-beam interferometer. A linearly polarised source is used, which couples to the two polarisation eigenmodes of a fibre with high linear birefringence. The two states of polarisation are now the equivalents of the signal and reference beams of the interferometer. The states propagate through the fibre, acquiring a measurand-dependent phase difference as described previously. Orthogonal states of polarisation do not interfere. Thus a polarisation analyser is used to resolve the two states into a common azimuth so that they interfere to produce the detected output intensity given by:

$$I = I_o(1 + V \cos \phi_2) \quad (12.9)$$

where ϕ_2 is the phase difference between the polarisation modes.

The similarity with Equation 12.7 is obvious. As before, the visibility depends on the relative intensities of the recombining modes. Optimum intensity and visibility are achieved by using a source polarised at $\pi/4$ radians to the eigenaxes of the fibre, and an analyser at $\pi/4$ to the eigenaxes at the output. Modified forms are available to give two antiphase outputs, of which the simplest merely replaces the output analyser with a polarising beamsplitter.

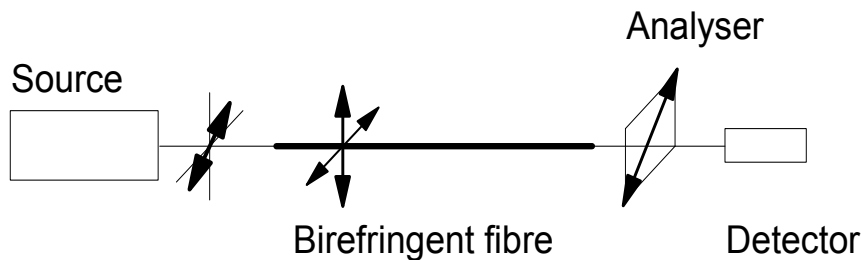


Figure 12.4 Simple polarimeter. The arrows indicate: the polarisation azimuth of the input beam; the directions of the eigenaxes of birefringence of the fibre; and the polarisation azimuth of the analyser.

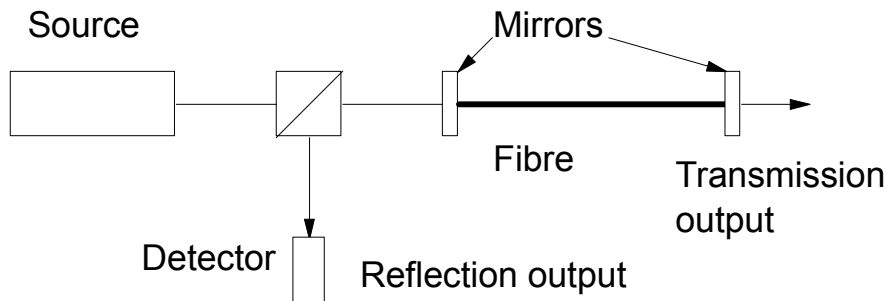


Figure 12.5 Fibre Fabry-Perot interferometer.

12.3.3 Multiple beam interferometers

So far we have considered only arrangements in which *two* beams interfere. However, multiple beam interferometry is also useful, and the most familiar form, the Fabry-Perot, with a fibre optic arrangement is shown in Figure 12.5. The transfer function is given by the well-known Airy function [23]

$$I = \frac{I_0}{1 + F \sin^2 \phi / 2} \quad (12.10)$$

where ϕ is the round-trip phase retardation and F is the finesse, which characterises the phase resolution of the device, where

$$F = 4R/(1 - R)^2 \quad (12.11)$$

where R is the mirror reflectance and attenuation is neglected.

The effect of the multiple transitions of the signal beam backwards and forwards between the mirrors that form the cavity is to increase the sensitivity. The higher the reflectivity of the mirrors, then the greater the number of circulations within the cavity that the beam can make before it is too greatly attenuated. Thus the finesse, reflectivity and sensitivity are related, as indicated in Figure 12.6.

There are obvious practical difficulties in depositing high-reflectivity mirrors onto the end-faces of fibres (although it can be done [24]), particularly if the coated fibre is then to be incorporated into a more extensive fibre system.

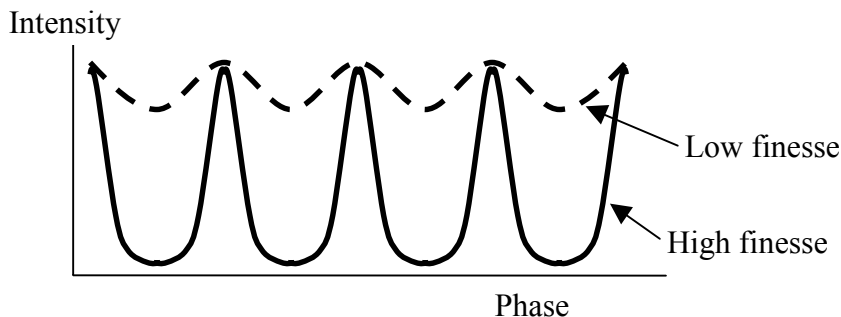


Figure 12.6 Transfer function in transmission for a Fabry-Perot interferometer.

In consequence, most fibre Fabry-Perot interferometers actually use low-reflectivity mirrors. A common form is simply to exploit the natural Fresnel reflection of about 4 % that takes place at the un-coated fibre-air interface. Under those circumstances, the transfer function is more like the low-finesse case shown in the diagram above. More recently, in-fibre Bragg gratings have begun to be used to define the mirrors to form the interferometer [25].

The extreme limit of low-finesse corresponds to two-beam interference, when the arrangement is more properly called a *Fizeau* interferometer. The Fizeau interferometer operated in reflection gives good visibility provided that the two reflections are of comparable intensity [26].

A multiple beam interferometer need not use any explicit reflections. A multiple beam interferometer related to the Sagnac arrangement is the ring-resonator, shown in Figure 12.7. Here, the beam propagates in only one direction, with a small fraction of the intensity coupling into an output port at each circulation. Thus, the interferogram is formed from successive circulations of the ring [27].

12.3.4 Dual wavelength interferometry

The periodicity of an interferogram is inherently one wavelength. An established technique to extend the range is to use two similar wavelengths [28]; the technique is often employed in fibre optical interferometry [29].

When a two-beam interferometer is illuminated by two monochromatic sources of wavelengths λ_1 and λ_2 , each of which alone would give a unit visibility interferogram of mean irradiance I_0 , then the observed irradiance is clearly

$$I = I_0 \left(1 + \cos \frac{2\pi nl}{\lambda_1} \right) + I_0 \left(1 + \cos \frac{2\pi nl}{\lambda_2} \right) \quad (12.12)$$

which may be rearranged to give

$$I = I_0 \left[1 + V \cos \left(\pi \cdot n \cdot l \frac{\lambda_1 + \lambda_2}{\lambda_1 \lambda_2} \right) \right] \quad (12.13)$$

where V is the fringe visibility, which may be found from

$$V = \cos \left[\pi \cdot n \cdot l \left(\frac{\lambda_2 - \lambda_1}{\lambda_1 \lambda_2} \right) \right] \quad (12.14)$$

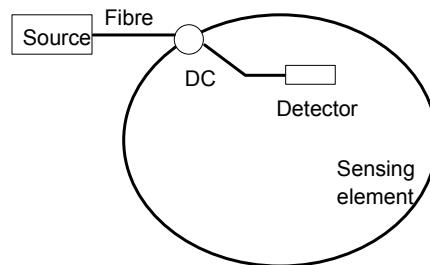


Figure 12.7 The fibre optic ring, resona-

Hence in such an arrangement, the resolution is equivalent to that in a single-wavelength interferometer. The unambiguous range is defined by the period of the visibility function, so that the dynamic range is increased by a factor of $\lambda_2/(\lambda_2-\lambda_1)$ in comparison with that obtained with the interferometer illuminated by λ_1 alone.

12.3.5 Low coherence interferometry

In an interferometer, fringes are visible only when the optical path difference is less than the coherence length of the beam at the detector, where the coherence length, l_c , is inversely proportional to the spectral width of the source, $\Delta\lambda$, thus $l_c \sim \lambda/\Delta\lambda$. Thus a typical diode laser source has a coherence length of tens of cm to m, whereas an LED may have a coherence length of tens to hundreds of μm . Thus when an interferometer is illuminated with a low-coherence source, it is possible to identify the position of zero Optical Path Difference (OPD) by looking for the highest visibility fringe [30]. It is therefore feasible to use coherence techniques to identify a unique reference OPD, and hence to overcome the fringe-order ambiguity inherent in interferometry.

It is possible to measure the OPD of a remote interferometer using a *tandem interferometer* arrangement [31], as shown in Figure 12.8. The sensing interferometer has an OPD greater than the source coherence length and no fringes are produced. Consider what happens as the OPD of the receiving interferometer is scanned. When its own OPD is zero, then fringes are observed. As the OPD is increased beyond the source coherence length, the fringes disappear. As the OPD is increased further to approach that of the sensing interferometer, then interference is possible between the pair of waves in which one takes the long path in the sensing interferometer and the short path in the receiving interferometer, and the other the short path in the sensing interferometer and the long path in the receiving interferometer; when the difference between the paths is less than the coherence length, then fringes are again observed. Thus fringe visibility shows a local maximum when the OPDs of the sensing and receiving interferometers match. It is then relatively straightforward to measure the OPD of the sensing interferometer separately in order to recover the measurand. A common technique is to use a separate high coherence source in the receiving interferometer, and to use conventional interferometry (e.g. counting fringes) to measure the distance between the zero OPD point and the path-matched OPD [32].

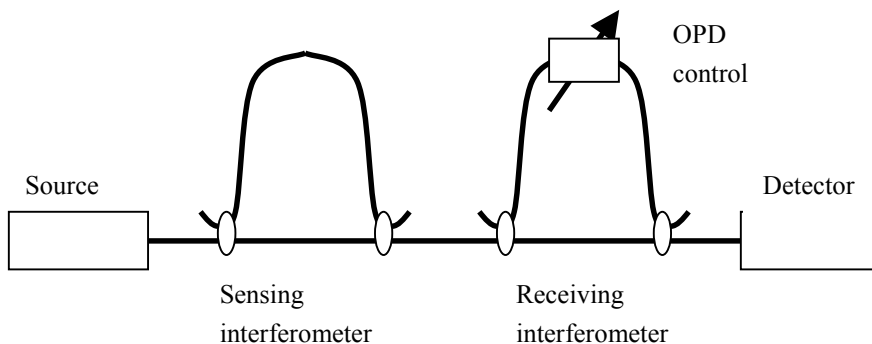


Figure 12.8 Tandem interferometry.

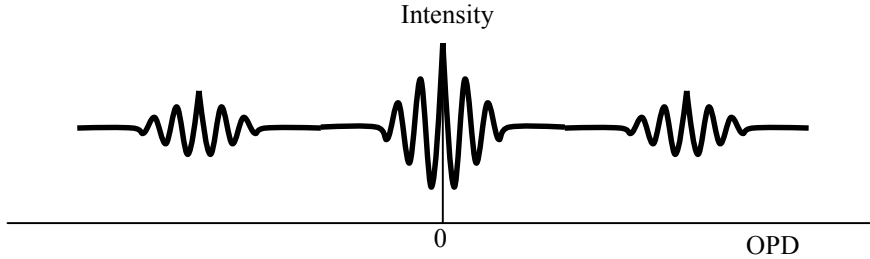


Figure 12.9 Schematic representations of interference fringes in tandem interferometry.

Practical schemes differ in the means used to scan the OPD and to analyse the interferograms produced. Path length scanning can use mechanical translation of the mirror in one arm of a bulk-optic receiving interferometer [33] or a shearing interferometer with an array detector such that the OPD is a function of position across the array [34]. An all-fibre technique that can give short scans involves using a travelling flexure wave in birefringent fibre to produce a travelling disturbance that couples light from the ‘fast’ to the ‘slow’ polarisation mode, thus changing its overall OPD [35]. For simple applications, analysis of the data need only be the identification of the central fringe. Higher performance can be achieved by capturing the complete interferogram and then using Fourier transform techniques to find the OPD [36] (Figure 12.9).

12.4 Phase Recovery

In most of the foregoing schemes, the signal recorded by the detector takes the form of Equations 12.7 and 12.8, i.e:

$$I = I_o[1 + V \cos(\phi_a - \phi_b)] \quad (12.15)$$

where ϕ_a and ϕ_b are the phases of the signal and reference beam. To visualise the problem of recovering the signal phase, consider the condition of a small harmonic signal $\phi_{ao} \sin \omega_a t$ superimposed on some large static phase shift which we shall include as part of ϕ_b .

Figure 12.10 shows (as expected) that the amplitude of the output intensity change for a given amplitude of phase signal is greatest where the transfer function is steepest, i.e. at position Q rather than position R . The position of greatest sensitivity corresponds to

$$\phi_a - \phi_b = \pi/4 + N\pi \quad (12.16)$$

the so-called *quadrature* condition, where N is an integer. In a practical interferometer, slowly varying changes in ϕ_b are inevitable due to environmental effects, so that the sensitivity of the interferometry would continually drift. Various techniques have been developed to recover the signal phase with constant sensitivity.

Homodyne techniques depend on controlling ϕ_b to maintain the quadrature position. The first of these, which is highly effective, was to actively control the phase in the reference arm of the interferometer by using a piezoelectric cylinder to stretch the fibre modulation [37]. An electronic servo loop applies a voltage to the cylinder to maintain the phase at a fixed value. If the bandwidth of the servo loop is wide enough to encompass the measurand, then the voltage applied to the modulator follows the signal.

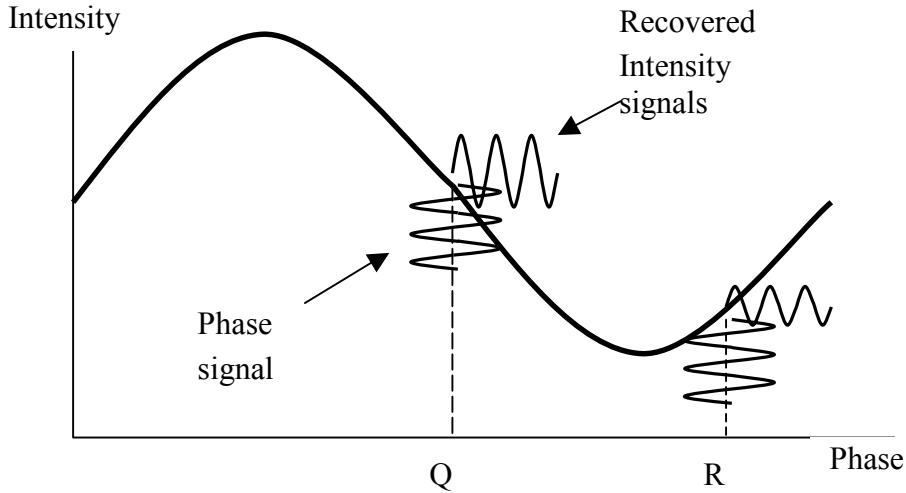


Figure 12.10 Recovery of harmonic phase signals.

For a low amplitude ($\ll 1$ rad), high frequency measurand it is often preferable to use a low-bandwidth servo loop to accommodate only the drift. Thus, at quadrature, the photodetector signal is proportional to the measurand, in the small angle approximation.

As an alternative to modulating the reference arm, it is possible instead to modulate the source wavelength, recalling that

$$\phi_a - \phi_b = 2\pi L / \lambda \quad (12.17)$$

where L is the OPD. This technique has been used to great effect with diode laser sources [38], where the wavelength can be modulated over a limited range by controlling the injection current [39]. Thus an arrangement can be constructed in which the feedback loop operates on the diode current rather than on an explicit phase modulator.

An interesting variant on this technique has been adopted for sensors based on in-fibre Bragg gratings (see Chapters 17 and 23). Here the measurand modulates the reflected wavelength. It is possible to use an unbalanced interferometer with a phase modulator and feedback loop to measure the wavelength, exploiting Equation 12.17; the changing wavelength is transduced to changing feedback voltage [40]. The sensitivity can be increased simply by using a longer OPD.

Passive phase recovery techniques are also possible, effectively the same as ‘phase stepping’ techniques that are used in full-field interferometry. They consist of deriving a sequence of outputs from the interferometer, where between each output the reference beam is ‘stepped’ by a known increment [41]. The simplest version to visualise generates four outputs separated by $\pi/2$ radians giving ideally:

$$I_i = I_o[1 + V \cos(\phi + i\pi/2)] \quad (12.18)$$

where $i = 1$ to 4, so that

$$\frac{I_3 - I_1}{I_4 - I_2} = \tan \phi \quad (12.19)$$

These passive techniques work particularly well with polarimetric sensors, where the phase

shift can be produced using a wave-plate. For example, consider the simple polarimetric sensor of Figure 12.4. Adding a quarter wave plate between the fibre and the output analyser would ‘step’ the phase by $\pi/2$ radians, provided that the eigenaxes of the wave plate were aligned with those of the fibre [42]. In interferometry, using a ‘3 by 3’ output coupler in the Mach-Zehnder arrangement provides three outputs, ideally separated by $2\pi/3$ radians [43].

Heterodyne schemes represent an alternative to homodyne ones. Here, a frequency shift is applied to the reference beam to produce a signal of the form

$$I = I_o[1 + V \cos(\phi_a - \phi_b - \omega_c t)] \quad (12.20)$$

producing the familiar form of the phase modulated carrier, which can be demodulated by a phase-locked loop or frequency discriminator. The practical difficulty is in producing the frequency shift. Bulk optic components, such as Bragg cells, can be used. Alternatives involve using periodic frequency shifts, e.g. using a piezoelectric fibre stretcher or by wavelength modulation of a diode laser by controlling its current in an unbalanced interferometer [44]. Various techniques have been reported involving gating and multiplication of the output [45,46]. Integrated optic phase shifters are also suitable. Research continues into all-fibre frequency shifting techniques [47]. Passive heterodyne processing may also be achieved by phase biasing, using the techniques described above [48].

The ultimate resolution with which phase may be recovered is normally limited by noise. The fundamental noise source is shot noise at the detector, set by the quantum nature of light and the Poissonian statistics of natural light sources, where the *shot noise* at the detector is [49]

$$I_{SN} = \sqrt{(2eI_o\Delta f)} \quad (12.21)$$

where Δf is the modulation bandwidth of the signal. However, in most situations the shot noise limit is not reached because of excess noise generated either by the source or the environment. The source imposes excess intensity and frequency noise. Intensity noise is relatively easily compensated. For example, having access to both antiphase outputs from an interferometer (see Equations 12.7 and 12.8) reveals both interferometer phase and source intensity [50]. Source frequency (wavelength) noise produces phase noise in the interferometer via Equation 12.17, which shows its effect to be directly proportional to the interferometer OPD [51]. In principle it is possible to use stabilisation or compensation techniques for frequency noise [52], but the usual approach is simply to minimise the OPD.

12.5 Multiplexing

In many situations, the decisive reason for using optical sensors is that it is possible to multiplex a set of sensing elements into a single measurement system (see Chapters 21 and 22). A discussion of multiplexing techniques [53] is beyond the scope of this chapter, but a few of the principal techniques will be mentioned here.

- a) **Time division:** the sensing elements are deployed along a single or multiple download/s such that when they are illuminated by a pulsed source, the returning pulses reach the common detector at distinct times, from which the individual sensor can be identified [54].

- b) **Wavelength division:** each sensor contains a spectrally-selective element, so that the signal from each sensor occupies a unique wavelength range. Thus by wavelength selection at the detector, the sensors can be identified.
- c) **Frequency division:** heterodyne processing is employed, where each sensor uses a different carrier frequency. Thus demodulation is achieved electronically [55,56].
- d) **Coherence division:** the sensors are illuminated by a low-coherence source. Each sensor has a different OPD, where all OPDs are greater than the coherence length, and differ from each other by more than the coherence length. Thus by using a tandem arrangement and scanning the OPD in the receiver interferometer it is possible to derive sequentially interferograms corresponding to each of the sensing interferometers [57]. A disadvantage is the substantial incoherent background inevitable as the number of sensors is increased.

12.6 Applications and Summary

The literature of interferometric and polarimetric sensors is now very extensive, and only the briefest indication of their range of applications can be given here. Probably the most useful, direct sensitivity of fibres, is to strain, and this has led to several important classes of sensor. The simplest of these are for the measurement of axial strain, where the most significant example is in structural monitoring. Fibre can be embedded into composite materials without compromising integrity. Long sensing lengths can be used to give a measurement integrated over a large system. Most often, multiplexed arrays are required to diagnose the state of the test object. A significant difficulty is to define sensing elements *inside* the test object, where for embedded systems it is obviously not possible to use components such as directional couplers. The advent of in-fibre Bragg gratings [58] to define reflectors in fibres has proved very useful for forming interferometers [59]. However, Bragg gratings make useful sensors on their own, and it is probably fair to say that for many structural monitoring applications involving large multiplexed arrays they are a more convenient design choice than the interferometer [60]. Nevertheless, there are some situations where interferometry is more appropriate. One example is the use of sensing elements to measure length changes in civil engineering structures. The sensing elements are essentially air cavities addressed by fibres, where the OPD changes in response to external dimensional changes [61]. The sensing elements are addressed by tandem interferometry to give absolute, high accuracy measurements. An advantage of using air-cavity sensors is that they avoid the temperature sensitivity inherent with fibres.

Fibre sensing elements are also capable of responding to transverse strain components. The application of transverse strain to a fibre induces linear birefringence; thus transverse strain measurement is polarimetric. This approach has been used most effectively with Bragg grating sensors in birefringent fibres to distinguish axial and transverse strain components [62,63].

Chapter 19 describes techniques for strain-temperature discrimination. However, in many situations the best approach is either to make a separate strain measurement, or to use common-mode rejection - i.e. to make *differential* strain measurements, where both sensing elements are exposed to the same temperature. An interesting example of common mode rejection occurs in the use of multicore fibre to measure bending. Each of the cores is used to form an interferometer. When the fibre is bent, the relative length of the cores changes, revealed as a phase change. Temperature affects each core equally and does not produce a phase shift [64,65].

The basic mechanisms for strain and pressure sensing are the same: physical changes in fibre dimensions and the strain-optic effect. By far the most important application of optical pressure sensing is for underwater acoustic measurements in hydrophones. Modern optical fibre hydrophones use coils of fibres on mandrels, air-backed or otherwise. The effect of pressure is to change the dimensions of the fibre and hence to modulate phase. Development programmes are far advanced with many examples of full-scale sea trials [66,67]. These sensors are always deployed in multiplexed arrays. Frequency, time and wavelength division have all been used.

The small size of optical fibres lends them to high spatial resolution and high resonant frequencies. One of the fastest pressure sensors reported is a miniature air-cavity terminated in a miniature metal diaphragm that also serves as a reflector to form an interferometer. The application of this instrument is in aerodynamics research, where \sim MHz bandwidths are required [68,69].

Many other measurands can be transduced to strain. An important early example was in sensitive measurements of magnetic fields. The primary sensing element is a magnetostrictive strip bonded to the fibre [70]. Thus the measurand magnetic field strains the fibre and so produces a phase change in the interferometer. The magnetostrictive effect is nonlinear, so that sensitivity is optimised by applying a bias field. By adding a harmonic 'dither field', the quasi-static measurand field is transduced to the frequency of the dither. Thus it is possible to distinguish the magnetic field from the effect of slowly-varying temperature [71]. Furthermore, by using different dither frequencies for different sensors, frequency division multiplexing is possible [72].

Optical techniques have considerable attractions for making measurements in high voltage systems, because of their intrinsically dielectric nature. Analogues of conventional voltage and current transformers have been developed, where the output is applied to a piezoelectric element which in turn strains a fibre [73]. Considerable development effort has been expended on direct measurements of magnetic and electric fields by magneto- and electro-optic effects [74]. As can be seen in Chapter 27 the most investigated systems have been based on the Faraday effect: in a medium, the polarisation azimuth of a beam is rotated by an amount proportional to the component of the magnetic field in the direction of the beam [75]. The Faraday effect in fused silica is small, but can be amplified by using a very long interaction path produced by coiling the fibre around the current-carrying conductor [76]. However, there are problems with other unwanted sources of birefringence, notably stresses induced by vibration [77]. Special fibres with higher sensitivity have been developed. Some successful systems use bulk-optic materials with high sensitivity as the sensing elements, addressed by fibres.

The intrinsic sensitivity of fibres to temperature is in most cases a disadvantage. However, it is of course useful in the measurement of temperature itself. The Bragg grating is in many cases a more appropriate technique: it is a simpler structure than an interferometer, demodulation is straightforward and there is no problem with fringe-order ambiguity [78]. However, for the highest resolution, interferometry is inevitably superior [79]. Thus interferometric sensors for special applications continue. Examples include miniature fibre Fizeau interferometers for turbomachinery measurements [80], based either on short fibre sensing elements [81,82], or coatings of high thermo-optic coefficient materials on the end faces of fibres [83]. In each case, μ m-scale spatial resolution has been achieved with bandwidths up to tens of kHz.

References

1. Jones, R.C. 'A new calculus for the treatment of optical systems', Parts I-III, *J. Opt. Soc. Am.*, 31, 488, 1941.
2. Hocker, G.B. 'Fibre optic sensing of pressure and temperature', *Appl. Optics*, 18, 1445, 1979.
3. Butter, C.D. and Hocker, G.B. 'Fibre optics strain gauge', *Appl. Optics*, 17, 2867, 1978.
4. Akhavan Leilabady, P., Jones, J.D.C. and Jackson, D.A. 'Single-mode fibre optic strain gauge with simultaneous phase- and polarization-state detection', *Optics Lett.*, 10, 576, 1985.
5. Corke, M., Kersey, A.D., Jackson, D.A. and Jones, J.D.C. 'All fibre "Michelson" thermometer', *Electron. Lett.*, 19, 471, 1983.
6. Giallorenzi, T.G., Bucaro, J.A., Dandridge, A., Sigel, G.H., Cole, J.H., Rashleigh, S.C. and Priest, R.G. 'Optical fibre sensor technology', *IEEE J. Quant. Electron.*, QE-18, 626, 1982.
7. Payne, D.N., Barlow, A.J. and Ramskov Hansen, J.J. 'Development of low and high birefringence optical fibres', *IEEE J. Quant. Electron.*, QE-18, 477, 1982.
8. Corke, M., Kersey, A.D., Liu, K. and Jackson, D.A., 'Remote temperature sensing using polarisation preserving fibre', *Electron. Lett.*, 20, 67, 1984.
9. Rashleigh, S.C. 'Polarimetric sensors: exploiting the axial stress in high birefringence fibres', *Proc. 1st Int. Conf. on Optical Fibre Sensors*, London: IEE, 221, 210, 1983.
10. Corke, M., Jones, J.D.C., Kersey, A.D. and Jackson, D.A. 'Combined Michelson and polarimetric fibre optic interferometric sensor', *Electron. Lett.*, 21, 148, 1985.
11. Farahi F., Webb D.J., Jones J.D.C. and Jackson D.A., 'Simultaneous measurement of temperature and strain: cross sensitivity considerations' *J. Lightwave Tech.* 8, 138 – 42, 1990.
12. Smith, A.M. 'Polarization and magneto-optic properties of single-mode optical fibre', *Appl. Optics*, 17, 52, 1978.
13. Langeac, D. 'Temperature sensing in twisted single-mode fibres', *Electron. Lett.*, 18, 1022, 1982.
14. Jackson D.A. and Jones J.D.C., 'Interferometers in Optical fibre sensors : systems and applications', Volume 2 (Ed B. Culshaw and J. Dakin) Artech House, Norwood MA,; p. 239-80, 1989.
15. Lefevre, H.C., 'Single-mode fibre fractional wave devices and polarization controllers', *Electron. Lett.*, 16, 778, 1980.
16. Anderson D. and Jones J. D. C. 'Optothermal frequency and power modulation of laser diodes' *J. Mod. Opt.* 39 1837 – 47, 1992.
17. Martinelli, M., *Opt. Comm.*, ~01.72, no.6, pp.341-4, Aug. 1989.
18. Lefevre, H. 'The Fibre Optic Gyroscope' Artech House, Boston, 1993.
19. Smith, R. B. 'Fibre optic gyroscopes: a bibliography of published literature' *Proc SPIE* 1585 464-503, 1991.
20. Akhavan Leilabady, P., Wayte, A.P., Berwick, M., Jones, J.D.C. and Jackson, D.A., 'A pseudo-reciprocal fibre optic Faraday rotation sensor', *Opt. Comm.*, 59, 173-6., 1986.
21. Harvey, D., McBride, R. and Jones, J. D. C. 'Fibre optic Sagnac interferometer based velocimeter' *Meas. Sci. Technol.* 3 1077–83, 1992.
22. Ulrich, R. 'Fibre-optic rotation sensing with low drift' *Opt. Letts.* 5, 173-5, 1980.
23. Born, M. and Wolf, E., 'Principles of Optics' (6th ed.), Pergamon, Oxford, 1986.
24. Stone, J., 'Optical fibre Fabry-Perot interferometer with finesse of 300', *Electron. Lett.*, 21, 504, 1985.
25. Henderson, P. J., Rao Y. J., Jackson, D. A., Zhang, L. and Bennion, I., 'Simultaneous multi-parameter monitoring using a serial fibre Fabry-Perot array with low coherence and wavelength domain detection' *Meas. Sci. Technol.* 9, 1837, 1998.
26. Kersey, A.D., Jackson, D.A. and Corke, M., 'A simple fibre Fabry-Pérot sensor', *Opt. Comm.*, 45, 71, 1983.
27. Tai, S., Kyuma, K., Hamanaka, K. and Nakayama, T., 'Applications of fibre optic ring using laser diodes', *Optica Acta*, 33, 1539, 1986.
28. Steele, W.H., 'Interferometry', *Cambridge Studies in Modern Optics*, Vol. 1, Cambridge University Press, 1983.
29. Kersey, A.D., Dandridge, A. and Burns, W.K., 'Two wavelength fibre gyroscope with wide dynamic range', *Electron. Lett.*, 22, 18, 1986.
30. Bosselmann, Th. and Ulrich, R., 'High-accuracy position-sensing with fiber-coupled white-light interferometers' 2nd International Conference on Optical Fibre Sensors (VDE-Verlag GmbH) Stuttgart, Eds. R. Th. Kersten and R. Kist, 361-4, 1984.
31. Lefevre, H C, 'White Light Interferometry in Optical Fiber Sensors' 7th International Conference on Optical Fibre Sensors (Institution of Radio and Electronic Engineers, Australia), Sydney, Eds S. Rashleigh, J. Love and S. Poole, 345-51, 1990.

32. Flavin, D. A., McBride, R., Greenaway, A. H., Burnett, J. and Jones, J. D. C., 'Combined temperature and strain measurement with a dispersive optical Fourier transform spectrometer' *Opt. Letts.* 19, 2167 – 70, 1994.
33. Wang, D. N., Ning, Y. N., Grattan, K. T. V., Palmer, A. W., and Weir, K.: *J. Lightwave Tech.*, Vol 12, 909-16, 1994.
34. Chen, S., Palmer, A. W., Grattan, K. T. V., Meggitt, B. T., and Martin, S.: *Electron. Lett.*, 2, No.12,1032-4, 1991.
35. Sinha, P. G., Kolltveit, E. and Blotekjzer, K., 'Two-mode fiber-optic time-delay scanner for white-light interferometry', *Electronics Letters*, vol. 20, no. 1, pp.94-6, Jan. 1995.
36. Flavin, D. A., McBride, R. and Jones, J. D. C., 'Interferometric fibre optic sensing based on modulation of group delay and first order dispersion: application to strain temperature measurand' *J. Lightwave Tech.* 13, 1314 – 23, 1995.
37. Jackson, D.A., Priest, R., Dandridge, A. and Tveten, A.B., 'Elimination of drift in a single-mode optical fibre interferometer using a piezo-electrically stretched coiled fibre', *Appl. Optics*, 19, 2926, 1980.
38. Jackson, D.A., Kersey, A.D., Corke, M. and Jones, J.D.C., 'Pseudo-heterodyne detection scheme for optical interferometers', *Electron. Lett.*, 18, 1081, 1982.
39. Dandridge, A. and Goldberg, L., 'Current induced frequency modulation in diode lasers', *Electron. Lett.*, 18, 302, 1982.
40. Koo, K.P. and Kersey, A. D. 'Fiber Laser Sensor System with Interferometric Read-Out and Wavelength Multiplexing' 10th International Conference on Optical Fibre Sensors, Glasgow 1994, eds. B. Culshaw and J. D. C. Jones *Proc SPIE* 2360, 331-4, 1994.
41. Creath, K., 'Temporal phase measurement methods', in *Interferogram Analysis*, D.W. Robinson and G.T. Reid (eds), IOP, Bristol, 1993.
42. Ren, Z.B. and Robert, Ph., 'Input polarization coding in fibre current sensors', *Springer Proceedings in Physics* 44, 261-6 1989.
43. Koo, K.P., Tveten, A.B. and Dandridge, A., 'Passive stabilization scheme for fibre interferometers using (3 × 3) fibre directional couplers', *Appl. Phys. Lett.*, 41, 616, 1982.
44. Jones, J.D.C., Corke, M., Kersey, A.D. and Jackson, D.A., 'A miniature solid-state directional laser Doppler velocimeter', *Electron. Lett.*, 18, 1081-3, 1982.
45. Cole, J.H., Danver, B.A. and Bucaro, J.A., 'Synthetic heterodyne interferometric demodulation', *IEEE J. Quant. Electron.*, QE-18, 694, 1982.
46. Kersey, A.D., Lewin, A.C. and Jackson, D.A. 'Pseudo-heterodyne detection scheme for the fibre gyroscope', *Electron. Lett.*, 20, 368, 1984.
47. C.N. Pannell, R.P. Tatam, J.D.C. Jones and D.A. Jackson, 'A fibre-optic frequency shifter utilising travelling flexure waves in birefringent fibre', *J. IERE*, (supplement on optical fibre components and networks), 58 S92-8, 1988.
48. Kersey, A.D., Corke, M. and Jackson, D.A. 'Linearized polarimetric optical sensor using a "heterodyne-type" signal recovery scheme', *Electron. Lett.*, 20, 209, 1984.
49. Conner, F. R., 'Noise' 2nd edition, Edward Arnold, 1982.
50. Dandridge, A. and Tveten, A.B., 'Noise reduction in fibre optic interferometric systems', *Appl. Optics*, 20, 2337, 1981.
51. Favre, F. and LeGuen, D., 'High frequency stability of laser diode for heterodyne communication systems', *Electron. Lett.*, 16, 179, 1980.
52. Cobb, K.W. and Culshaw, B., 'Reduction of optical phase noise in semiconductor lasers', *Electron. Lett.*, 18, 336, 1982.
53. Kersey, A.D. and Dandridge, A., 'Comparative analysis of multiplexing techniques for interferometric fiber sensing', *Fiber Optic and Laser Sensors*, SPIE vol. 1120, pp. 236-46, 1989.
54. Dakin, J., Wade, C.A. and Henning, M.L., 'Novel optical fibre hydrophone array using a single laser source and detector', *Electron. Lett.*, 20, pp.53-4, 1984.
55. Dandridge, A., Tveten, A.B., Kersey, A.D. and Yurek, A.M., 'Multiplexing of interferometric sensors using phase generated carrier techniques', *J. Lightwave Tech.*, vol. LT-5, no. 7, pp. 947-52, 1987.
56. Santos, J.L., Farahi, F., Newson, T., Leite, A.P. and Jackson, D.A., 'Frequency multiplexing of remote all-fiber Michelson interferometers with lead insensitivity', *J. Lightwave Tech.*, 10, 6, pp. 853-63, 1992.
57. Farahi, F., Newson, T.P., Jones, J.D.C. and Jackson, D.A., 'Coherence multiplexing of remote fibre optic Fabry-Perot sensor system', *Opt. Comm.*, 65, 319-21, 1988.
58. Hill, K. O., Fujii, Y., Johnson, D. C. and Kawasaki, B. S., 'Photosensitivity in optical fiber waveguides: Application to reflection filter fabrication', *Appl. Phys. Lett.*, 32, 10, pp. 647-9, 1978.
59. Rao, B. S. J., Jackson D.A., 'Recent progress in fibre-optic low-coherence interferometry', *Meas. Sci. Technol.*, 7, pp.98 1-999, 1996.
60. Measures, R. M., Alavie, T., Maaskant, R., Huang, S., and LeBlanc, M., 'Bragg grating fiber optic sensing for bridges and other structures', *Second European Conference on Smart Structures and Materials*, Proceedings of the SPIE, Vol. 2361, pp.

- 162-7, 1994.
61. Inaudi, D., Elamari, A., Pflug, L., Gisin, N. Breguet, J. and Vurpillot, S., 'Low-coherence deformation sensors for the monitoring of civil-engineering structures', *Sensor and Actuators A*, 44, 125-30, 1994.
 62. Udd, E., Nelson, D. V. and Lawrence, C. M., 'Three Axis Strain and Temperature Fiber Grating Sensor', *Proceedings of SPIE*, 2718, p. 104, 1996.
 63. Lawrence, C. M., Nelson, D. V. and Udd, E., 'Measurement of Transverse Strains with Fiber Bragg Gratings', *Proceedings of SPIE*, 3042, p. 218, 1997.
 64. Gander, M. J., Macrae, D., Galliot, E. A. C., McBride, R., Jones, J. D. C., Blanchard, P. M., Burnett, J. G. and Greenaway, A. H., 'Two-axis bend measurement using multicore optical fibre' *Opt Comm* 182, 115-21, 2000.
 65. Gander, M. J., MacPherson, W. N., McBride, R., Jones, J. D. C., Zhang, L., Bennion, I., Blanchard, P. M., Burnett, J. G. and Greenaway, A. H., 'Bend measurement using Bragg gratings in multicore fibre' *Electron Lett.* 36, 120-1, 2000.
 66. Nash, P.J. and Cranch, G.A., 'Multi-channel optical hydrophone array with time and wavelength division multiplexing', *Proc. 13th Conf. Optical Fibre Sensors*, SPIE vol. 3746, pp. 304-7, Kyongju, Korea, April 12-16, 1999.
 67. Davis, A.R., Kirkendall, C.K., Dandridge, A. and Kersey, A.D., '64 channel all optical deployable acoustic array', *Proc. 12th Conf. Optical Fibre Sensors*, Technical Digest, Post conference Edition. Opt. Soc. America, Washington, DC, USA, pp. 616-19, 1997.
 68. MacPherson, W. N., Kilpatrick, J. M., Barton, J. S. and Jones, J. D. C., 'Miniature fibre optic pressure sensor for turbomachinery applications' *Rev. Sci. Inst.* 70, 1868-74, 1999.
 69. MacPherson, W. N., Gander, M. J., Barton, J. S., Jones, J. D. C., Owen, C. L., Watson, A. J. and Allen, R. M., 'Blast-pressure measurement with a high-bandwidth fibre optic pressure sensor' *Meas. Sci. Technol.* 11, 95-102, 2000.
 70. Koo, K.P. and Sigel, G.H., 'Characteristics of fibre optic magnetic field sensors employing metallic glasses', *Optics Lett.*, 7, 334, 1982.
 71. Kersey, A.D., Corke, M., Jackson, D.A. and Jones, J.D.C., 'Detection of DC and low frequency AC magnetic fields using an all single-mode fibre magnetometer', *Electron. Lett.*, 19, 469, 1983.
 72. Kersey, A.D., Jackson, D.A. and Corke, M., 'Single-mode fibre optic magnetometer with DC bias field stabilization', *IEEE J. Lightwave Technol.*, LT-3, 836, 1985.
 73. Jackson, D. A., Ning, Y. N., McGarrity, C., and Santos, J. L. 'Three Phase Current Measurement Using A Hybrid Current Sensing Technique' *Proc 8th Optical Fibre Sensors Conference*, Monterey CA, Eds. F. Leonberger and A. Dandridge (IEEE Catalog #92CH3107-0), 1992.
 74. Bosselmann, T., 'Electric and Magnetic Field Sensing for high Voltage applications', *Optical Fibre Sensors Technologies and Applications SPIE Proc.* 3097, 1997.
 75. Smith, A. M. 'Optical fiber current measurement device at a generating station', 1980 European Conference on Optical Systems and Applications, Utrecht, SPIE Vol. 236, pp. 352-7, 1980.
 76. Day, G. W. and Rose, A. H., 'Faraday Effect Sensors: The State of the Art', *Fiber optic and Laser Sensors VI*, Boston, SPIE Vol. 985, pp. 138-51, 1988.
 77. Rogers, A. J., *J. of Optoelectronics*, 3,391, 1988.
 78. Rao Y J, Webb D J, Jackson D A, Zhang L and Bennion I, 'In-tibre Bragg grating temperature sensor system for medical applications' *J. Lightwave Technol.* 15, 779-85, 1996.
 79. Farahi, F., Jones, J. D. C. and Jackson, D. A., 'High speed fibre optic temperature sensor' *Opt. Letts.* 16, 1800 - 2, 1991.
 80. Kidd, S.R., Sinha, P.G., Barton, J.S. and Jones, J.D.C., 'Interferometric fibre sensors for measurement of surface temperature heat transfer rates on turbine blades' *Opt. and Laser Eng.* 16, 207 -21, 1992.
 81. Inci, M. N., Kidd, S. R., Barton, J. S. and Jones, J. D. C., 'Fabrication of single mode fibre optic Fabry Perot interferometers using fusion spliced titanium dioxide coatings' *Meas. Sci. Technol.* 3, 678 - 84, 1992.
 82. Kidd, S. R., Barton, J. S., Inci, M. N. and Jones, J. D. C. 'Unsteady gas temperature measurement using an ultra-short optical fibre Fabry Perot interferometer' *Meas. Sci. Technol.* 5, 816 - 22, 1994.
 83. Kidd, S. R., Barton, J. S., Meredith, P., Jones, J. D. C., Cherrett, M. A. and Chana, K. S. 'A fibre optic probe for gas total temperature measurement in turbomachinery' *International Gas Turbine and Aeroengine Congress and Exposition*, 94-GT-34, The Hague, 13 - 16 June 1994.